ELSEVIER

Polymer Degradation and Stability 71 (2001) 15–30

Polymer Degradation and Stability

www.elsevier.nl/locate/polydegstab

The wear-out approach for predicting the remaining lifetime of materials

Kenneth T. Gillen *, Mat Celina

Sandia National Laboratories, Albuquerque, NM 87185-1411, USA

Received 20 May 2000; accepted 20 June 2000

Abstract

Failure models based on the Palmgren–Miner concept that material damage is cumulative have been derived and used mainly for fatigue life predictions for metals and composite materials. We review the principles underlying such models and suggest ways in which they may be best applied to polymeric materials in temperature environments. We first outline expectations when polymer degradation data can be rigorously time–temperature superposed over a given temperature range. For a step change in temperature after damage has occurred at an initial temperature in this range, we show that the remaining lifetime at the second temperature should be linearly related to the aging time prior to the step. This predicted linearity implies that it should be possible to estimate the remaining and therefore the service lifetime of polymers by completing the aging at an accelerated temperature. We refer to this generic temperature-step method as the ''wear-out'' approach. We next outline the expectations for wear-out experiments when time–temperature superposition is invalid. Experimental wear-out results are then analyzed for one material where time–temperature superposition is valid and for another where evidence suggests it is invalid. In analyzing the data, we introduce a procedure that we refer to as time–degradation superposition. This procedure not only utilizes all of the experimental data instead of a single point from each data set, but also allows us to determine the importance of any ''interaction effects''.

Keywords: Polymers; Aging; Cumulative damage; Lifetime predictions; Remaining life

1. Introduction

Given the importance of predicting polymer lifetimes in critical applications (e.g. defense applications, nuclear reactor safety components, aircraft components), considerable effort has been devoted to developing improved accelerated aging methods [1]. Most accelerated aging approaches first expose unaged material to various accelerated environments and then measure and model the changes that occur in the material. The goal is to extrapolate the accelerated results obtained in order to predict the material lifetime under ambient aging conditions. In the best situation, if material is available that has been ambiently aged for a significant period of time, the properties of this material can be used to check the extrapolated predictions.

In addition to this obvious application of ambiently aged material, it would be advantageous to have a methodology for using this resource to estimate the material's remaining lifetime in the ambient environment. If sacrificial samples of ambiently aged material could be used to estimate their remaining lifetimes, then more confidence would exist in any accelerated aging predictions. One promising technique, which we refer to as the ''wear-out'' approach, is based on the well-established, Palmgren–Miner concept that degradation is cumulative [2,3] and that failure is therefore considered to be the direct result of the accumulation of damage with time. In this report, we review the principles underlying this wear-out approach and show how they can best be applied to polymeric materials in temperature environments.

2. Experimental

2.1. Materials

Nitrile rubber-compression-molded sheets (~2-mm thick) of a typical commercial nitrile rubber formulation

* Corresponding author. Tel.: +1-505-844-7494; fax: +1-505-844-9781.

E-mail address: ktgille@sandia.gov (K.T. Gillen).

0141-3910/01/$ - see front matter
PII: S0141-3910(00)00112-9

[100 parts Hycar 1052 resin, 65 pph (of resin) N774 carbon black, 15 pph Hycar 1312, 5 pph zinc oxide, 1.5 pph 2246 (hindered phenol) antioxidant, 1.5 pph sulfur, 1.5 pph MTBS, 1pph stearic acid] were obtained from Burke Rubber Co.

EPDM elastomer-compression-molded sheets (~2 mm thick) of a compound designated SR793B-80, an EPDM that was specially formulated for this study, were obtained from Sargent Rubber Co. It contains 100 parts Nordel 1440 (a terpolymer of ~53% ethylene, 47% propylene and 3% 1,4 hexadiene), 40 pph N-990 carbon black, 25 pph N-539 carbon black, 5 pph Zipstick 85, 12 pph DiCup 40C and 10 pph SR-350 (co-curing agents) and 2 pph Flectol H antioxidant.

2.2. Oven aging

Oven aging of the compression molded sheet materials and the oxygen consumption cells was carried out in air-circulating ovens (±1°C) equipped with thermocouples connected to continuous strip chart recorders.

2.3. Tensile tests

Tensile samples (~150 mm long by 6 mm wide by ~2 mm thick) were cut from the compression molded sheets before aging. Tensile testing (5.1 cm initial jaw separation, 12.7 cm/min strain rate) was performed on an Instron 1000 tensile testing machine equipped with pneumatic grips; an extensometer clamped on the sample allowed ultimate tensile elongation values to be obtained.

2.4. Oxygen consumption measurements

Oxygen consumption rates were measured using a technique that has been described in detail elsewhere [4]. This technique monitors the change in oxygen content caused by reaction with polymer in sealed containers using quantitative gas chromatographic analyses.

2.5. Density measurements

Density measurements were made using the Archimedes approach [5,6], where the sample (typically 50 mg) is weighed in air and then in ethanol on a balance with a reproducibility of better than 10 micrograms.

2.6. Modulus profiles

Modulus profiles with a resolution of ~50 μm were obtained on sample cross-sections using a computer-controlled, automated version of our modulus profiling apparatus, which has been described in detail previously [7]. This instrument measures inverse tensile compliance, which is closely related to the tensile modulus.

3. Results and discussion

3.1. Accelerated aging and the time-temperature superposition approach

The approach normally used to accelerate the oxidative aging of polymers is to raise the air-oven aging temperature, thereby increasing the rates of the oxidative reactions which often dominate the degradation. The reactions underlying oxidative degradation of elastomers can be extremely complex and usually have not been worked out in detail. Fortunately, variants [8] of the basic autoxidation scheme (BAS), derived many decades ago by Bolland [9], Bateman [10] and co-workers for the homogeneous oxidation of liquid hydrocarbons, have proved to offer reasonable approximations to the degradation of many polymers [1,4]. For illustrative purposes, we will use the simplified scheme shown below; it represents a first approximation for the oxidation of stabilized polymers containing antioxidants (AH).

$$\text{Polymer} \xrightarrow{k_1} \text{R}^\bullet$$

$$\text{R}^\bullet + \text{O}_2 \xrightarrow{k_2} \text{RO}_2^\bullet$$

$$\text{RO}_2^\bullet + \text{RH} \xrightarrow{k_3'} \text{RO}_2\text{H} + \text{R}^\bullet$$

$$\text{RO}_2\text{H} + 2\text{RH} \xrightarrow{k_4} 2\text{R}^\bullet + \text{ROH} + \text{HOH}$$

$$\text{RO}_2^\bullet \xrightarrow{k_5=k_5'[\text{AH}]} \text{Products}$$

$$\text{R}^\bullet \xrightarrow{k_6=k_6'[\text{AH}]} \text{Products}$$

Analysis of this kinetic scheme under steady-state conditions for $\text{R}^\bullet$, $\text{RO}_2^\bullet$ and RO_2H leads to

$$\frac{\text{d}[\text{O}_2]}{\text{d}t} = \frac{C_1[\text{O}_2]}{1 + C_2[\text{O}_2]} \tag{1}$$

where C_1 and C_2 are constants involving several of the kinetic rate constants [1,4].

The first important conclusion from the result shown in Eq. (1) is that such kinetic analyses predict a constant rate of reaction under constant temperature conditions. This turns out to be a reasonable approximation for many stabilized polymers. As an example, Fig. 1 shows some representative isothermal oxygen consumption rate results versus aging time for the nitrile [4,11] material. For this plot, the arrows pointing to the data at 96 and 80°C correspond to the approximate aging times required at these temperatures for the ultimate tensile elongation to reach 10% of its initial value. If we arbitrarily define 10% of initial elongation as the material's mechanical lifetime, these results show that the oxygen consumption rate is relatively constant over the entire

mechanical degradation lifetime. Changing the aging temperature clearly leads to approximately multiplicative changes in the constant oxidation rate. A reasonable assumption in polymer aging is the expectation that an equivalent amount of oxidation at two different temperatures leads to equivalent mechanical damage. Given the multiplicative change in oxidation rates, this implies that mechanical degradation curves at different constant temperatures should have approximately the same shape when plotted versus the log of the aging time. Results consistent with such expectations can be seen in Fig. 2, which shows normalized elongation results (elongation divided by the elongation for the unaged material) for the nitrile rubber material aged at five temperatures.

The most common method of analyzing aging data, such as that shown in Fig. 2, involves first choosing some arbitrary failure criterion, for instance the time for the elongation to reach 25% of its initial value. The values of the failure time at each temperature can then be used to test various aging models. For instance, the commonly used Arrhenius model assumes that an activated chemical process with activation energy E_a determines the temperature dependence of k, the rate of degradation, i.e.

$$k \propto \exp\left(\frac{-E_a}{RT}\right) \tag{2}$$

Determining whether a plot of the log of the failure time versus inverse absolute aging temperature yields linear results can serve as a test of this model. Unfortunately, the above procedure uses only one processed data point from each curve, eliminating most of the experimental points from analysis. However, if a constant multiplicative factor relates the time dependencies of two temperature curves, then the same functional relationship between time and temperature will hold regardless of where on the degradation curve one chooses to analyze. Thus, if the results give Arrhenius behavior at 25% of initial elongation, they should follow the same Arrhenius relationship at 50, 75%, etc. (linear with the same slope).

A better approach to test for the presence of constant multiplicative factors and to determine the relationship between time and temperature involves the time–temperature superposition concept [1,12]. For this approach, we first select the lowest experimental temperature (e.g. 64.5°C for the data shown in Fig. 2) as the reference temperature. Then, for each set of data at a higher temperature T, we multiply the experimental times at this temperature by a constant shift factor, a_T, chosen empirically to give the best overall superposition with the reference temperature data ($a_T = 1$ at the reference temperature). Fig. 3 shows the results of applying this procedure to the elongation data of Fig. 2, where the bottom x-axis gives the superposed results at the reference temperature of 64.5°C. The excellent superposition that occurs is not surprising, given the earlier observation that the raw experimental results at the various temperatures had similar degradation shapes when plotted versus the log of the aging time. The next step is to determine whether a simple model can be used to explain the relationship between the empirically determined shift factors and the temperature. The commonly used Arrhenius functionality of Eq. (2) would predict that

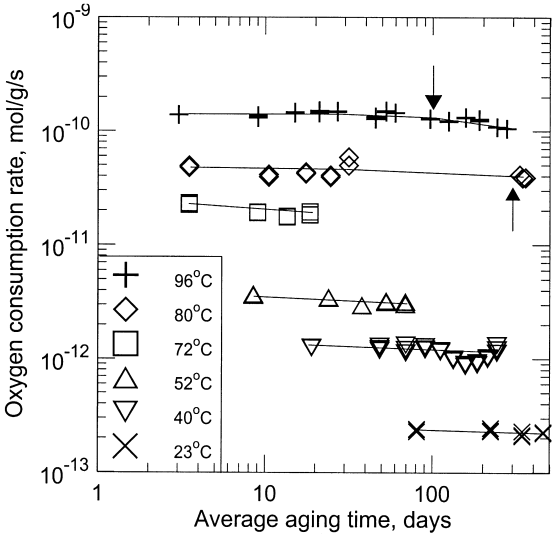

Fig. 1. Oxygen consumption rates for the nitrile rubber material versus aging time at the indicated temperatures. Arrows indicate the approximate times at the two highest temperatures where the elongation reaches 10% of its initial value.

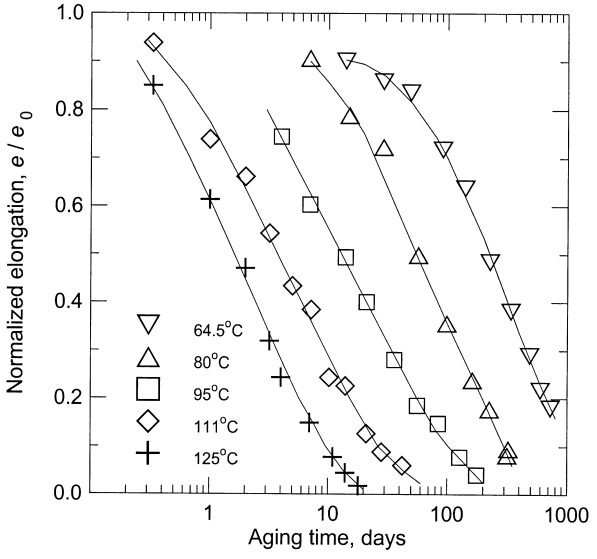

Fig. 2. Normalized elongation results for the nitrile rubber versus aging time at the indicated temperatures.

$$a_T = \exp\frac{E_a}{R}\left(\frac{1}{T_{ref}} - \frac{1}{T}\right) \quad (3)$$

If Arrhenius is valid, a plot of the log of the a_T values versus the inverse absolute temperature should give linear behavior. Fig. 4 shows that the elongation results for a_T (the crosses on the solid line) are consistent with the Arrhenius assumption, with E_a ~90 kJ/mol, determined from the slope of the line through the results.

To make predictions below the lowest experimental temperature (64.5°C; $a_T = 1$), the normal procedure would be to extrapolate the result. As an example, the dashed line in Fig. 4 shows such an extrapolation for the nitrile data. The extrapolated a_T would be ~0.014 at around 25°C, which would imply that this material would last ~70 times longer at this temperature compared to its lifetime at 64.5°C. A refined extrapolation (solid line) based on the use of ultrasensitive oxygen consumption measurements down to room temperature [4] is also shown in this figure. This extrapolation indicates an a_T of approximately 0.02 at 25°C, predicting a room temperature lifetime ~50 times longer than at 64.5°C. Predictions based on this latter extrapolation are indicated by the top x-axis in Fig. 3.

It is important to note that, unlike the normal Arrhenius testing procedure that may use only one processed data point from each curve, the time–temperature superposition procedure uses all of the raw data generated for a material. When time–temperature superposition is confirmed, strong evidence therefore exists for a constant acceleration in all of the main reactions underlying degradation.

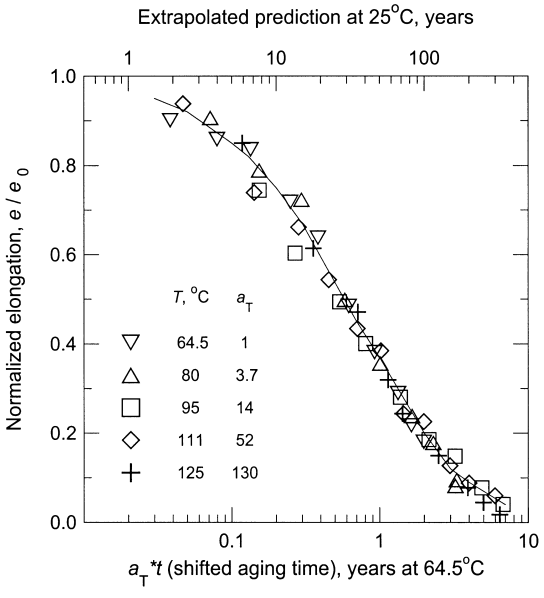

Fig. 3. Empirical time–temperature superposition of the nitrile data from Fig. 2 at a reference temperature of 64.5°C (lower x-axis). The upper x-axis shows predictions resulting from an extrapolation of the 64.5°C superposed results to 25°C.

3.2. Wear-out approach for predicting remaining lifetime

The wear-out approach is based on the simple concept that degradation is cumulative and that failure is therefore considered to be the direct result of the accumulation of damage with time. Models based on this concept have been largely confined to fatigue life predictions for metals and composite materials. A typical analysis begins by assuming that fatigue damage is being induced by applying a dynamic stress level r under constant frequency, temperature, moisture content, etc., conditions [13]. In this case the damage D can be written as a function of the applied stress level r and the number of fatigue cycles, n

$$D = F(n, r) \quad (4)$$

Assuming that N_i represents the number of cycles necessary to reach failure under a given constant amplitude loading condition r_i and that the damage function D starts at 0 (where $n = 0$) and reaches unity at failure (where $n = N_i$), a simple case occurs when

$$D = F(n, r_i) = f(n/N_i) \quad (5)$$

for any value of r_i. This case is referred to as a "stress-independent damage model" since the same curve will represent the relationship between D and n/N_i independent of the value of r_i. A particularly simple case occurs when the damage is linearly related to n/N_i, a situation shown as the solid line in Fig. 5. This line is labeled P–M, since the earliest fatigue damage models used by Palmgren [2] and Miner [3] assume such linear behavior.

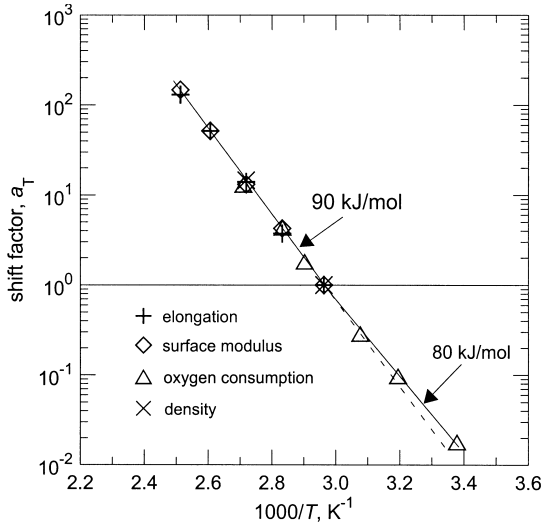

Fig. 4. Arrhenius plot of shift factors obtained from empirical time–temperature superposition of the indicated nitrile rubber degradation parameters.

For most real damage parameters, damage will not accumulate linearly, implying more complex damage accumulation curves. Hypothetical examples are shown by the dashed curves labeled 1, 2, and 3 on Fig. 5. Curve 3, for instance, would represent so-called induction–time behavior, in which the damage remains relatively unchanged until just before failure, where it begins to accumulate rapidly. Whatever the shape of the damage curve, whenever a stress-independent damage model holds, the same curve (e.g. curve 3 in Fig. 5) will describe the change of the damage parameter versus n/N_i, regardless of the value of r_i.

It turns out that the presence of time–temperature superposition for thermal aging of polymers is conceptually equivalent to the so-called "stress-independent damage model" used above. Instead of the damage being described generally as a function of the stress amplitude r and the number of fatigue cycles n, the damage will be given by

$$D = F(t, T) \tag{6}$$

where the aging time t replaces n and the temperature T replaces r. With τ_i representing the time to reach failure at a given temperature T_i, the case of a "stress-independent damage model" leads to

$$D = F(t, T_i) = f(t/\tau_i) \tag{7}$$

We found above that the elongation results for thermally aged nitrile rubber (Fig. 2) led to excellent time–temperature superposition (Fig. 3). If we arbitrarily define failure of the elongation as the time required for the elongation to decrease to 20% of its original value, the data of Fig. 2 can be used to estimate values of the failure times τ_i versus temperature. The results are 700, 200, 54, 15 and 5.6 days at 64.5, 80, 95, 111 and 125°C, respectively. When the elongation results at each temperature are then plotted versus t/τ_i, excellent superposition (stress-independent damage) occurs as shown in Fig. 6. This is essentially the same superposed data shown in Fig. 3, except for several minor differences. First of all, instead of a log time scale, it is plotted on a linear time scale, consistent with damage accumulation discussions. Also consistent with damage accumulation ideas, the data terminate at the failure criterion of 20% of initial elongation (the right-hand axis shows the damage function D going from 0 at the top to 1 at the bottom). Finally, the data analyzed in terms of t/τ_i result in superposed data that, from a time–temperature superposition point-of-view, have slightly different shift factors (shown on Fig. 6) from the results shown in Fig. 3. This is because truncated data (down to the failure criterion) were superposed in Fig. 6 whereas the complete data set was superposed in Fig. 3. The top axis of Fig. 6 shows the superposed time axis in years at 64.5°C corresponding to the bottom t/τ_i axis, obtained from the τ_i values relative to the value of 700 days at the 64.5°C reference temperature.

Now that it is obvious that time–temperature superposition is equivalent to the concept of a stress-independent damage function, we can see that the fatigue-related lower x-axis of Fig. 5 can be replaced by an axis involving t/τ_i for thermally induced chemical degradation cases (upper x-axis in Fig. 5). In fact it is clear that the nitrile experimental elongation data given in Fig. 6

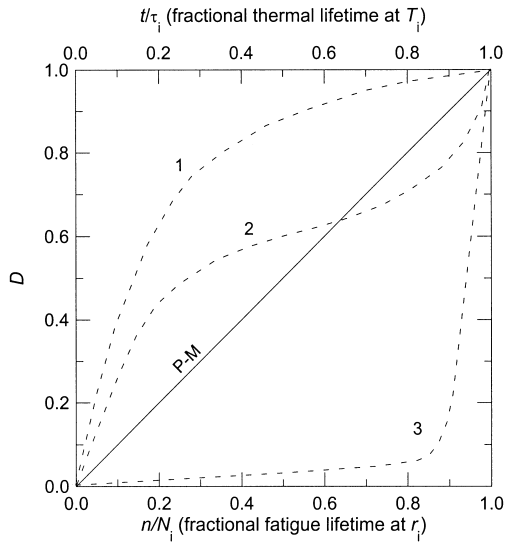

Fig. 5. Schematic showing some representative relationships between degradation parameters and fractional fatigue lifetime (lower x-axis) or, equivalently, fractional thermal lifetime (upper x-axis).

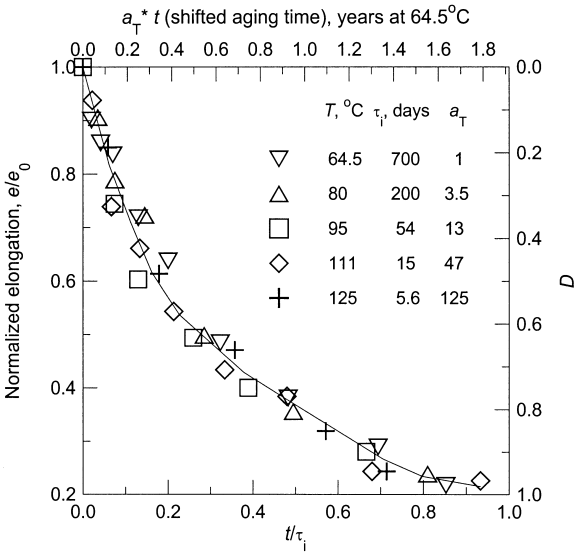

Fig. 6. Normalized elongation results for the nitrile rubber material (left y-axis) versus fractional thermal lifetime (lower x-axis) for the indicated temperatures. The right y-axis shows the degradation variable, whereas the top x-axis shows the time-temperature superposed data at a reference temperature of 64.5°C.

represent a degradation variable whose functional dependence on time is similar to curve 1 of Fig. 5 (in this case inverted due to the manner in which D is plotted). For the simplest situation, the degradation variable would be linearly related to time, as indicated by the solid curve labeled P–M in Fig. 5. We showed earlier (Fig. 1) that the oxidation rate for the nitrile is found to be relatively constant throughout the mechanical property lifetime. This implies that the underlying degradation chemistry is also relatively constant (linear) versus time. Unfortunately, the mechanical degradation variables of typical interest (e.g. elongation, tensile strength) are usually related in a complex, non-linear manner to the underlying chemistry, implying non-linear time–dependence even in the presence of "linear" chemistry. Whatever the shape of the damage curve, however, whenever time-temperature superposition holds (stress-independent damage model), the same curve will describe the change of the damage parameter versus fractional degradation lifetime, regardless of the temperature (Fig. 6).

We now examine a situation where we raise the temperature T_i part way through the material's degradation from T_1 to a higher wear-out temperature $T_{w,}$ whose purpose is to complete the aging of the material (hence the name wear-out temperature). We define t_1 as the time spent at T_1 and determine the "wear-out" time t_w subsequently required at T_w to reach failure. For any damage parameter that gives time–temperature superposition, a reasonable assumption is that the degradation level (given by the chemical changes in the material) is identical for identical values of the damage parameter regardless of the temperature used to reach this level. For such situations, the same curve will continue to be traversed independent of when the temperature is stepped from T_1 to T_w and it is easy to see from Fig. 5 that in general

$$\frac{t_1}{\tau_1}+\frac{t_w}{\tau_w}=1 \tag{8}$$

regardless of the shape of its damage curve versus the fractional degradation lifetime.

This relationship for a step change in temperature from T_1 to T_w (or the reverse) is plotted as the solid line in Fig. 7 (bottom x-axis and left y-axis). Defining $a_{w,1}$ as the shift factor relating the two temperatures,

$$a_{w,1}=\frac{\tau_1}{\tau_w} \tag{9}$$

and combining with Eq. (8) gives

$$t_w=\frac{\tau_1-t_1}{a_{w,1}}, \tag{10}$$

which predicts a linear relationship between t_w and t_1. This relationship can also be represented by the solid line (labeled I) in Fig. 7, using the upper x-axis together with the right-hand y-axis, where the time on each axis runs from 0 to the failure time. We will refer to behavior described by Eq. (10) as linear wear-out behavior to distinguish it from the Palmgren–Miner linear damage behavior (line marked P–M in Fig. 5), since the latter is not required for the former. The parameter $a_{w,1}$ can be thought of as the "acceleration factor" for the Wear-out approach.

The situation becomes more complex when time–temperature superposition is invalid. An example is shown in Fig. 8, where hypothetical data for a normalized degradation variable (e.g. tensile elongation) are plotted versus log time at temperatures T_1 and T_2. It is clear that the shapes of the degradation curves at T_1 and T_2 are different, implying that the acceleration factor relating the degradation at the two temperatures depends on the damage level. For this example, the values of a_T become larger (note representative values on figure) as the amount of degradation increases, corresponding to a "spreading-out" of the lower temperature results. If we arbitrarily choose the failure criterion

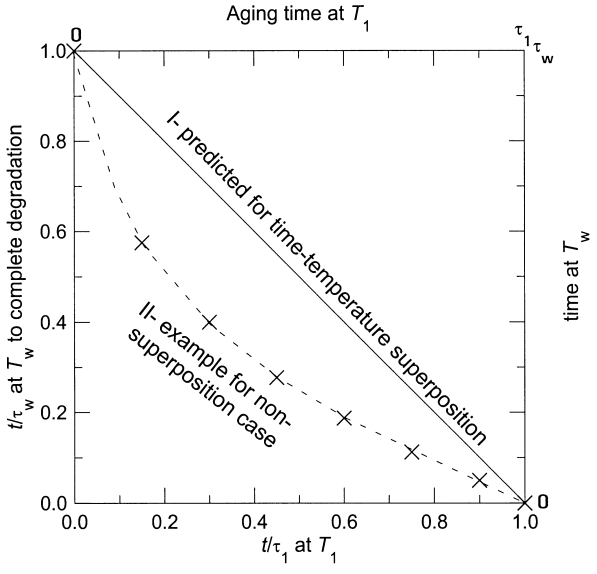

Fig. 7. Hypothetical wear-out plots showing predictions when time–temperature superposition is valid (solid line labeled I) and an example when superposition is invalid (dashed curve labeled II through points from Table 1).

Table 1
Theoretical wear-out results derived from Fig. 9

t_1/τ_1	0	0.15	0.3	0.45	0.6	0.75	0.9	1
t_w/τ_w	1	0.575	0.4	0.277	0.187	0.112	0.05	0

as a 90% loss in the degradation variable and replot these two curves versus their normalized aging times (aging time divided by failure time), the results are shown in Fig. 9 as the two solid curves.

Suppose wear-out experiments are performed on this hypothetical material. We will first assume that the value of the degradation variable determines the chemical degradation state regardless of how the sample reached this state. In other words, it is assumed that the chemical makeup of the sample is equivalent, as long as the value of the degradation variable is identical. This implies that stepping of the temperature to T_2 after a certain amount of aging time at T_1 will involve a horizontal shift from the T_1 curve to the T_2 curve. As an example, if the sample was exposed to T_1 until t/τ_1 reached 0.3, then the temperature was stepped to T_2, the degradation pathway would first follow the T_1 curve, then switch horizontally to the T_2 curve as indicated by the arrows on Fig. 9. After the step, the degradation will follow the T_2 curve until failure, again as indicated by the arrows along this curve. For this latter part of the wear-out experiment, t/τ_2 starts at ~ 0.6 and failure is reached when t/τ_2 reaches 1.0 which implies that $t_w/\tau_w \sim 0.4$. In a similar fashion, values of t_w/τ_w corresponding to other values of t_1/τ_1 can be generated; representative pairs are shown in Table 1. When we plot the results from this table on Fig. 7 (crosses), we see that non-linear wear-out behavior is predicted. For the case shown (Fig. 9), where the relative degradation rate at the wear-out temperature starts out slower but later accelerates compared to the situation at T_1, the shape of the wear-out results will be similar to the dashed curve (labeled II) drawn through these data. Thus, if the shapes of both curves are known (e.g. Fig. 9) and the chemical state of the material on both curves is assumed to be equivalent for equivalent values of the degradation variable, the exact shape of the wear-out curve can be predicted. We will use this procedure to make model predictions for some real elongation data below. In general, when the data spreads out as shown in Fig. 8, the predicted wear-out results will follow a curve similar to curve II of Fig. 7, where the slope of the curve will decrease with level of degradation. This situation will result in conservative lifetime predictions if data from early wear-out results are linearly extrapolated to the x-axis.

A more complex situation exists if the same level of degradation at the two temperatures does not correspond to equivalent material damage (e.g. the composition of chemical degradation products is different). In this case, the degradation rate after the temperature is stepped to T_2 may not be the same at the same level of the degradation variable as for a sample aged only at T_2. An example of this so-called "interaction" effect is shown in Fig. 10, where the degradation rate after the step (dashed curve) is greater than predicted in the absence of interaction. Such interaction effects will normally result in non-linear wear-out behavior. However, in contrast to the cases described above, the shape of the wear-out curve cannot be predicted, even when the shapes of the individual curves are known.

3.3. Wear-out example when superposition appears to be valid — nitrile material

We saw earlier that the nitrile material had excellent time–temperature superposition for its elongation data (Fig. 3) from 125°C down to 64.5°C, with shift factors that followed an Arrhenius dependence with temperature (Fig. 4). In addition, the oxygen consumption

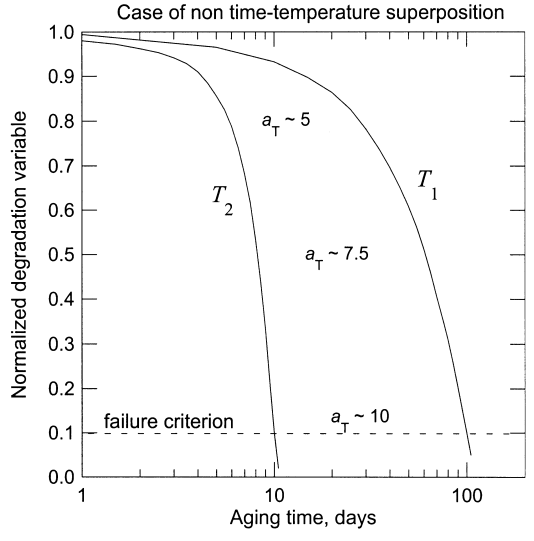

Fig. 8. Hypothetical example of a degradation property that does not time–temperature superpose.

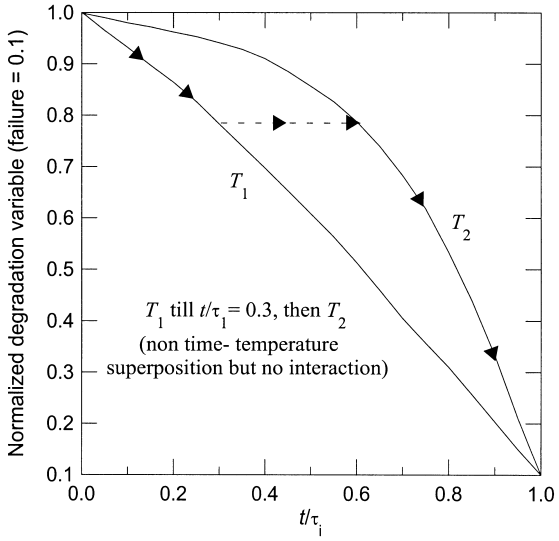

Fig. 9. The non-superposable results from Fig. 8 plotted against fractional thermal lifetime. A hypothetical wear-out experiment is shown by the arrows assuming no interaction.

results for this material were approximately constant versus time at all temperatures (Fig. 1) from 95°C down to room temperature and time–temperature superposed with shift factors that gave Arrhenius behavior similar to the elongation results (Fig. 4). These results suggest that time–temperature superposition should hold for this material from 125°C down to room temperature. This implies that approximately linear wear-out behavior might be expected for this material. Therefore, if we had some of this nitrile material that had been previously aged at room temperature for extended periods of time (tens of years), we could test the wear-out ideas outlined above by completing the aging at an elevated temperature. Unfortunately, such samples do not exist. We do, however, have a series of samples that have aged for periods of time ranging up to two years at 64.5°C (see Fig. 2) and we will use these samples to test the wear-out concept by completing their degradation at 95°C.

In order to test wear-out ideas, we need to select a wear-out degradation parameter. An immediate complication occurs for the nitrile material since previous work has shown that important diffusion-limited oxidation (DLO) effects [4,11] influence its thermoxidative degradation. At equilibrium in air environments, oxygen is dissolved in polymeric materials; its concentration is given by the product of the oxygen partial pressure surrounding the material and the solubility coefficient for oxygen in the material. DLO effects occur if oxidation reactions use up the dissolved oxygen faster than it can be replenished by diffusion from the surrounding air atmosphere. This leads to a drop in the oxygen concentration in the interior of the material, potentially leading to reduced or non-existent oxidation in these regions. The importance of such effects will depend primarily on three factors: the oxygen permeability coefficient (equal to the product of solubility and diffusivity), the rate of oxygen consumption and the material thickness [11,14,15]. It turns out that such DLO effects are quite often observed for polymers under typical accelerated aging conditions [4,11,16]. There are many experimental methods that can be used to screen for such effects [17]. One of the most useful for elastomers is modulus profiling [7], which involves an instrument that allows the modulus to be quantitatively mapped (typical experimental scatter of ±5%) across the cross-section of a material with a resolution of approximately 50 μm. Fig. 11 shows modulus profiles across the 2-mm thick nitrile rubber material after aging for various times at the four highest accelerated aging temperatures [11]. The *x*-axis variable, *P*, gives the percentage of the distance from one air-exposed surface to the opposite air-exposed surface. At the highest aging temperature of 125°C, important DLO effects cause highly heterogeneous degradation to occur. Oxidative hardening (modulus increases) is important at the sample surface, but becomes much less important in the interior regions. As the temperature is lowered, the rate of oxygen consumption goes down faster than the oxygen permeation rate, leading to reductions in the importance of DLO. At the lowest temperature of 64.5°C, where DLO effects are no longer important, the degradation gives steady homogeneous increases in modulus [11]. Besides various experimental methods capable of monitoring DLO effects, it is now possible to theoretically model DLO and therefore estimate its importance before any accelerated aging experiments are initiated [11,14,15].

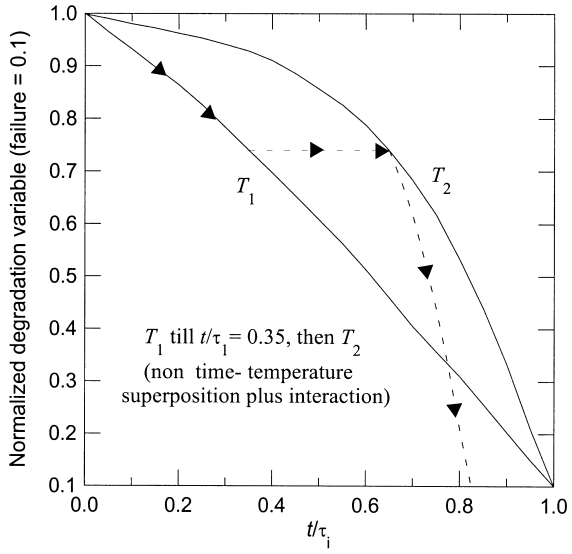

Fig. 10. The non-superposable results from Fig. 8 plotted against fractional lifetime. A hypothetical wear-out experiment is shown by the arrows assuming interaction.

Given the importance of DLO for the aging of the nitrile material, and its complex dependence on temperature, it is perhaps surprising that the elongation results for this material display both excellent time–temperature superposition and Arrhenius behavior. This turns out to be due to a fortunate circumstance, which occurs for the elevated temperature oxidation of many elastomeric materials [11]. As shown in Fig. 11, the oxidative hardening is greatest at the sample surfaces, where the oxidation is independent of DLO effects. During tensile testing, cracks would be expected to initiate at the hardened surface. If such cracks immediately propagate through the rest of the material, the ultimate tensile elongation will be directly dependent on the true, equilibrium (non-DLO influenced) oxidation. This turns out to be the case for many but not all materials where oxidative hardening dominates the degradation. Time–temperature superposition of the surface modulus results for the nitrile material leads to shift values (the diamonds in Fig. 4) virtually identical to those found for the elongation results, consistent with this picture.

We therefore conclude that DLO effects can complicate analyses of degradation properties that are sensitive to the entire sample cross-section (e.g. tensile strength at break), but may have no effect on properties that are either measured at the sample surface or are determined by the surface properties (elongation). Elongation would therefore be a viable degradation property to follow during wear-out testing. Unfortunately, elongation measurements are destructive and even a single measurement requires a large amount of material (experimental scatter usually dictates a minimum of three repeat measurements for each aging time). As we will show below, wear-out experiments require that the degradation parameter of interest be followed until its failure criterion is reached; a typical experiment might require six aging times at the wear-out temperature. Thus for each aging time at 64.5°C, a large quantity of elongation samples (on the order of 20) would have to be wear-out aged at 95°C. If such large quantities of "ambiently-aged" materials are not available (as is the case for the nitrile samples preaged at 64.5°C), alternative degradation parameters must be chosen.

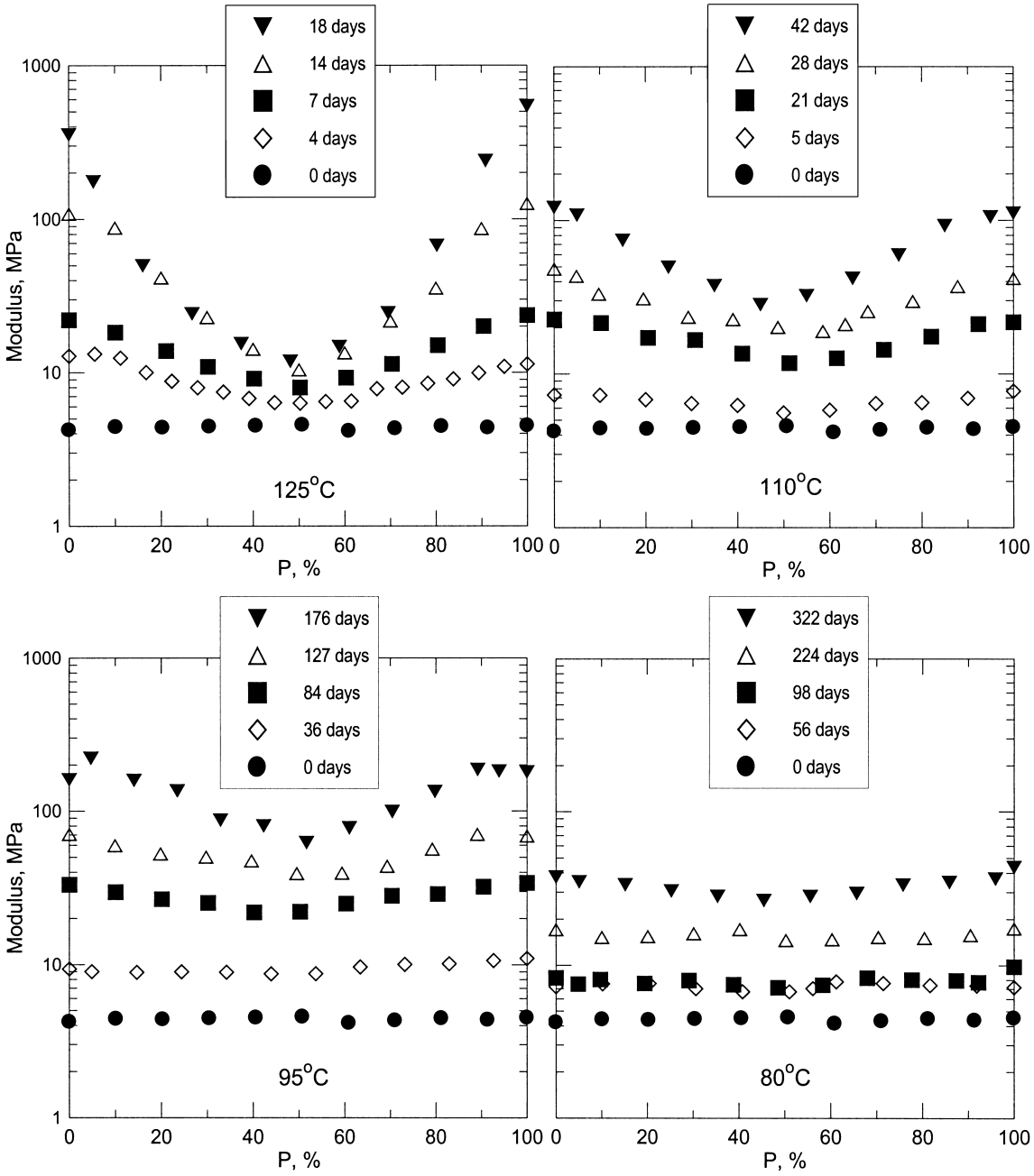

Fig. 11. Modulus profiles versus aging time and temperature for the 2-mm thick nitrile rubber. P denotes the percentage of the distance from one air-exposed sample surface to the opposite air-exposed surface.

Because of the small samples required for measurement and the expected sensitivity to oxidative degradation, we decided to investigate density as the wear-out degradation parameter for the present study. Recent evidence suggests that density may be one of the most universally applicable parameters for following degradation dominated by oxidation effects both in thermo-oxidative and radiation environments [18]. One of the most important reasons for density increases is the replacement of hydrogen along chains by much heavier oxygen-containing species. In addition, many commercial polymers have high-density fillers such as carbon black (density ~1.81 g/cc) and clay (density ~2.5 g/cc). Fractional reductions in the much lower density polymer component, through loss of gaseous polymer degradation products (e.g. CO_2, CO, H_2O), will increase the relative weighting of the high density fillers, and therefore lead to increases in sample density.

To determine the sensitivity of density to degradation in the nitrile material, we conducted density measurements on the samples aged at 64.5°C. At this temperature, modeling indicates that the integrated oxidation is ~97% of a homogeneously oxidized sample [11], implying minimal DLO effects. The density results at 64.5°C, which are plotted in Fig. 12, show an approximately linear increase with aging time, confirming the viability of density as a degradation parameter for this material. Since similar modeling predicts [11] that moderate DLO effects will occur for 2-mm thick sheet material at the wear-out temperature of 95°C, we reduced the size of the 64.5°C preaged samples by cutting them into ~2-mm cubes. For 95°C wear-out aging of these smaller samples, the integrated oxidation will be greater than 96% of a homogeneously oxidized sample, again minimizing DLO effects. Density results for unaged 2-mm cubes exposed versus time to a 95°C environment are shown in Fig. 12. The slope of the line through the 95°C data is 14.6 times that of the line through the 64.5°C data. Since this shift factor for density is consistent with the shift factors for elongation, oxygen consumption and surface modulus (all are plotted in Fig. 4), it is clear that the density correlates with the other degradation parameters.

Fig. 13 shows the density results versus 95°C aging time for ~2-mm cubic samples that had previously been aged for the indicated number of days at 64.5°C. Earlier in Fig. 6, we arbitrarily defined failure as the time required for the elongation to decrease to 20% of its original value. By comparing the elongation results of Figs. 2 and 3 with the density results shown in Fig. 12, we note that density values reaching ~1.24 g/cc are approximately consistent with the $e/e_0 = 0.2$ failure criterion. Using this density as the failure criterion, the values of t_w required at 95°C for density failure are obtained versus the 64.5°C aging time from Fig. 13. The results are plotted as diamonds on the wear-out plot shown in Fig. 14. As anticipated, the results are reasonably linear and offer some early evidence of the applicability of wear-out ideas.

A better method of analyzing the wear-out results of Fig. 13 involves a procedure that we define as "*time-degradation superposition*", in which the wear-out density curves are shifted to a reference state with an additive shift factor defined as a_D. When density wear-out results are available for initially unaged material, these data (the solid circles in Fig. 13) are selected as the reference state ($a_D = 0$). If time–temperature superposition is valid, the shapes (on a linear time plot) of the degradation curves during the high temperature (95°C) exposures should be identical. Thus by attempting time–degradation

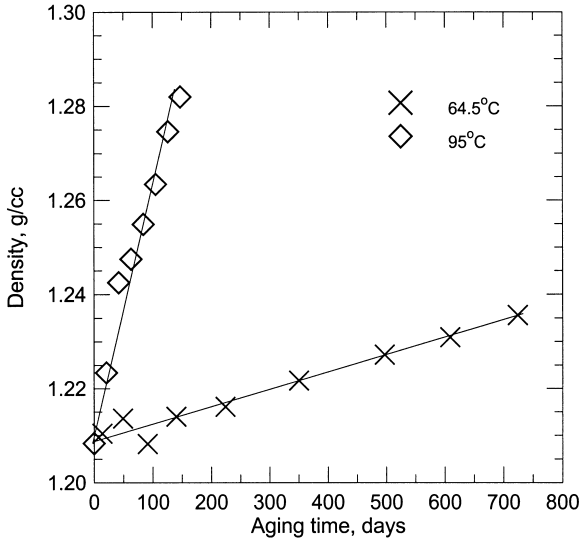

Fig. 12. Density results for aging of 2-mm thick nitrile samples at 64.5°C and ~2-mm cubic nitrile samples at 95°C.

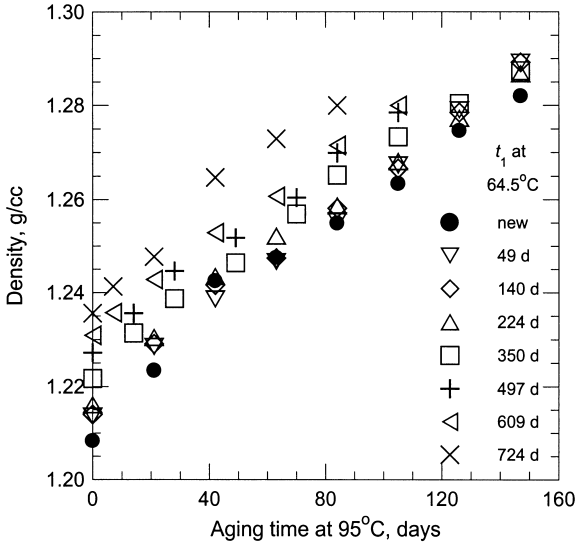

Fig. 13. Density results versus aging time at 95°C for the nitrile samples previously aged at 64.5°C for the indicated times.

superposition, we are able to test the assumptions underlying time–temperature superposition. In addition, this procedure uses all of the wear-out data instead of just a single processed point (e.g. the time required to reach a density of 1.24 g/cc).

Fig. 15 shows the results obtained from applying the time–degradation superposition procedure to the data of Fig. 13. It is clear that reasonable time-degradation superposition exists for this data, not surprising given the similar shapes observed for the different sets of data on Fig. 13. The empirically derived additive shift factors (designated as a_D) that lead to the best superposition are indicated on Fig. 15, where the reference condition ($a_D = 0$) corresponds to the previously unaged material. An important advantage of the time–degradation superposition approach is that a defined failure criterion is not required. In order to use the shift factors for predicting remaining lifetime, however, a failure criterion must obviously be selected. If, for instance, we again select 1.24 g/cc as the failure criterion, the superposed results of Fig. 15 indicate that 51 d at 95°C is required to reach this condition for the previously unaged material. If we define t_{95} as the time required from the time–degradation superposed curve to reach our selected failure criterion (1.24 g/cc), then the effective wear-out time t_W is given by

$$t_W = t_{95} - a_D \tag{11}$$

Therefore, a plot of $51 - a_D$ versus aging time at 64.5°C would represent a wear-out plot from time–degradation superposition that is equivalent to the failure time plot (diamonds in Fig. 14). The distinction would be that the experimental data come from time–degradation superposition (all of the data used) instead of from single processed points (the estimated failure times). The results of this procedure are plotted as open squares in Fig. 14. Again the results are reasonably linear with perhaps slightly less scatter than those obtained from a single point on each wear-out curve. The lines drawn through the two sets of data intersect the x-axis at ~810 and 865 days, respectively. These extrapolations predict that ~840 days would be required at 64.5°C for the material density to reach 1.24 g/cc, a value consistent with the 840 day value found by a slight linear extrapolation of the 64.5°C results shown in Fig. 12.

In an actual application, the wear-out approach would be used to first test for and then extrapolate linear behavior for predicting the remaining lifetime of a material. We can get a flavor of how this procedure would work by assuming failure of the nitrile corresponds to a more severe elongation drop of 90% to 10% of initial, a level not attained after 2 years of aging at 64.5°C (Fig. 2). Comparing the 95°C results from Figs. 2 and 12, we see that $e/e_0 = 0.1$ corresponds to the density reaching ~1.26 g/cc. From the superposed time–degradation results of Fig. 15, we determine that ~94 days at 95°C are required to reach this density, so we can now plot $94 - a_D$ versus the aging time at 64.5°C on our wear-out plot (solid squares in Fig. 14). These data, based on the time–degradation superposition analyses clearly represent a simple upward shifting of the open squares by 43 units (94–51). The line through these data can then be extrapolated to the x-axis, leading to a prediction of ~1470 days (4.02 years) for the density to reach ~1.26 g/cc (and therefore the elongation to reach ~10% of initial) at 64.5°C. This extrapolated prediction from wear-out results compares favorably to the ~3.8 years predicted from analyses of time-temperature superposed accelerated elongation data (Fig. 3).

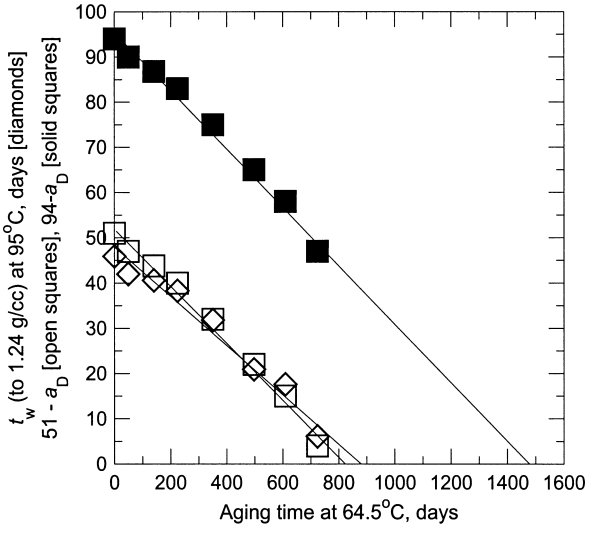

Fig. 14. Experimental wear-out results for the nitrile material. Samples previously aged at 64.5°C were wear-out aged at 95°C.

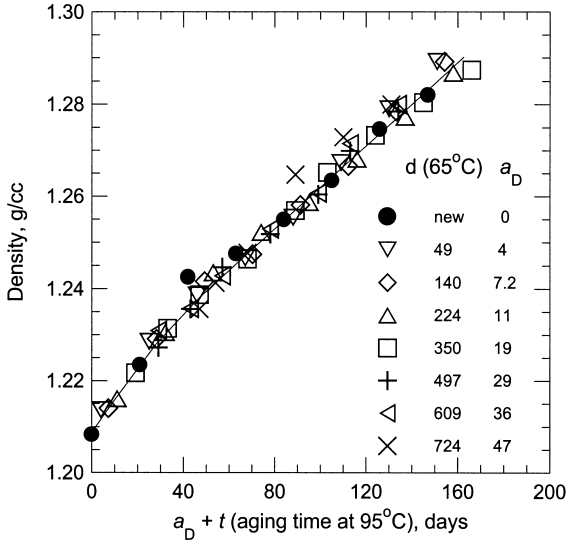

Fig. 15. Time–degradation superposition of the nitrile density results shown in Fig. 13.

3.4. Wear-out example when superposition appears to be invalid — EPDM material

Ultimate tensile elongation results versus aging time for an EPDM material at four temperatures, ranging from 111 to 155°C, are shown in Fig. 16. It is clear that, at each temperature, the elongation drops rather abruptly, corresponding to so-called "induction-time" behavior and therefore curve 3 of Fig. 5. At first glance, the curves at the four temperatures have reasonably similar shapes, suggesting that time–temperature superposition of the data may be applicable and this assumption is preliminarily confirmed by the superposed results shown in Fig. 17 (the shift factors used to superpose the results are indicated in the figure). However, a closer look at the results shown in Figs. 16 and 17 suggests that the drop in elongation occurs somewhat less abruptly at 111°C. This in turn suggests that a change in oxidation mechanism may occur around this temperature.

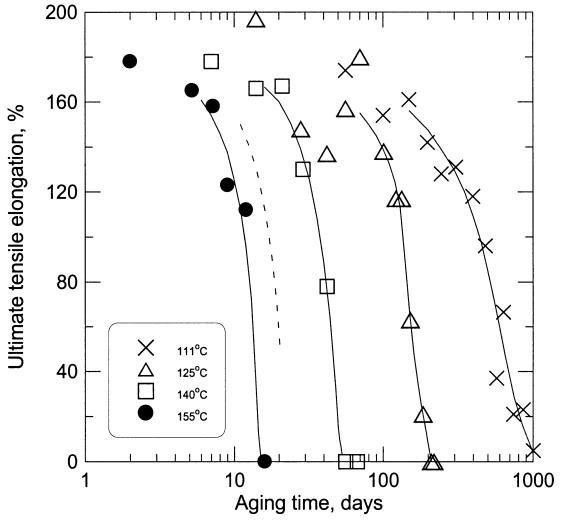

Fig. 16. Elongation results versus time and temperature for the EPDM material together with interpolated results at 150°C (dashed curve).

Oxygen consumption results taken over a much larger temperature range (160 down to 52°C) are shown in Fig. 18. In general, the consumption rates tend to decrease somewhat with time at every temperature. When measurements are taken past the "induction time", there is a rapid increase in oxidation rate as evidenced by the rapid increase at 125°C beyond ~150 days (Fig. 16 shows that the elongation decreases rapidly around this same time). We integrate the data shown in Fig. 18 and then time–temperature superpose the resulting oxygen consumption curves at a reference temperature of 111°C (this reference temperature allows us to compare shift factors with those from elongation shown in Fig. 17). The superposed oxygen uptake results are shown in Fig. 19, where the experimentally determined shift factors a_T for oxygen consumption are indicated on the figure. The resulting oxygen consumption shift factors are plotted (Fig. 20) on an Arrhenius plot (log of a_T versus inverse absolute temperature) together with the shift factors determined from elongation (Fig. 17). Above 111°C, the oxygen consumption shift factors are consistent with those from elongation establishing strong evidence that the oxidation reactions being followed with the consumption measurements are responsible for the changes in elongation. Below 111°C, the activation energy for oxygen consumption begins to drop implying a change in oxidation mechanism must be occurring around 111°C. This evidence supports the earlier elongation evidence that also suggested a change in degradation mechanism around 111°C.

With the above evidence that the 111°C elongation data does not superpose with higher temperature

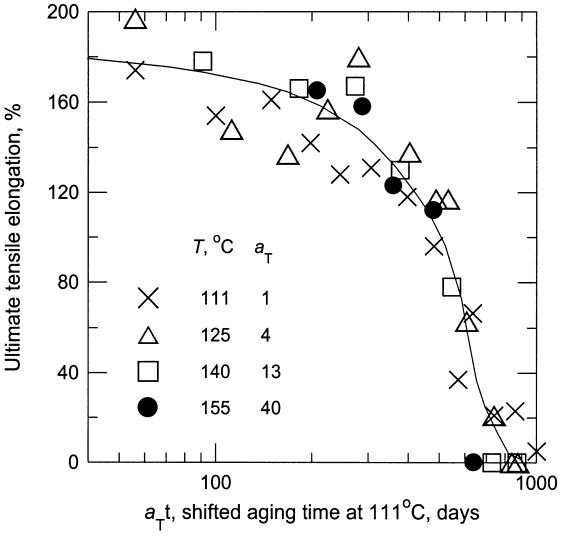

Fig. 17. Time–temperature superposition of the EPDM elongation results shown in Fig. 16.

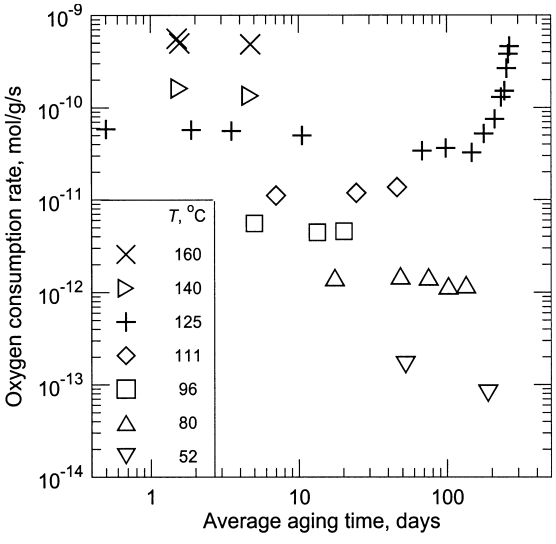

Fig. 18. Oxygen consumption rate results for the EPDM material versus time at the indicated temperatures.

results, we decided to use samples from the 111°C aging series to test the wear-out approach for a non-superposition case by completing the aging of these samples at 150°C. Assuming that 50% absolute elongation corresponds to "failure", we find from the 111°C elongation plot (Fig. 16) that failure occurs after ~620 days. At 150°C (dashed line on Fig. 16 resulting from interpolating between the 140 and 155°C curves), failure takes ~20.5 days. These two data points represent the intersection points on the x and y axes, respectively, of a wear-out plot. Since the 111°C elongation results change shape (non-superposition) relative to the higher temperature results, we would expect a non-linear wear-out curve connecting these points for samples previously aged at 111°C. Assuming no interactions occur (the value of the degradation variable determines the chemical degradation state regardless of how the sample achieved this state), we can theoretically model the shape of the Wear-out curve. We use the same procedure outlined above that generated the theoretical Wear-out results of Table 1 (plotted in Fig. 7) from the hypothetical data given in Fig. 9. We do this using the smooth curve drawn through the 111°C data in Fig. 16 together with the smooth dashed curve derived at 150°C. The resulting predictions are shown by the dashed curve drawn on Fig. 21.

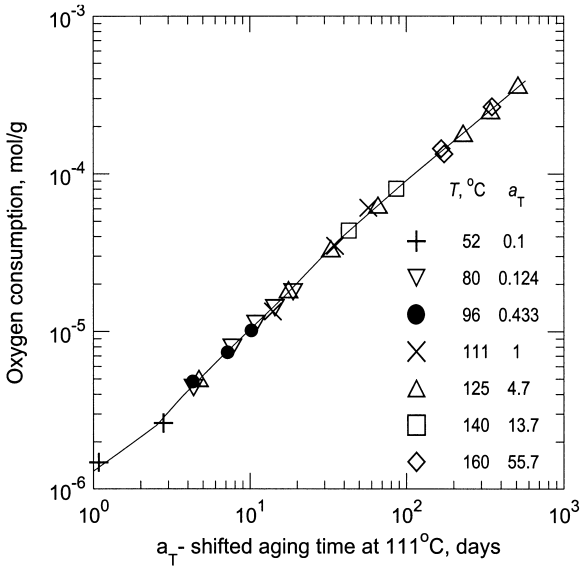

Fig. 19. Time–temperature superposition of the integrated oxygen consumption results derived from the oxygen consumption rate data of Fig. 18.

We now have to select a degradation parameter to use for the wear-out experiments. It turns out that all of the candidate parameters for this material (elongation, density, modulus, swelling) show "induction-time" behavior, where changes are small until the induction time but rapid thereafter. When trying to determine the condition of a material in the field, induction-time behavior represents a significant challenge since measurements of material properties versus aging time may give little warning of an impending catastrophic failure. This situation, therefore represents one of the most attractive applications of the wear-out approach, since a catastrophic failure with no warning may be able to be transformed into wear-out results that may change in a more predictive manner.

As an example of the induction-time behavior for this material, Fig. 22 shows density results versus time and temperature. Since density can be measured quickly and accurately on relatively small samples, we decided to use

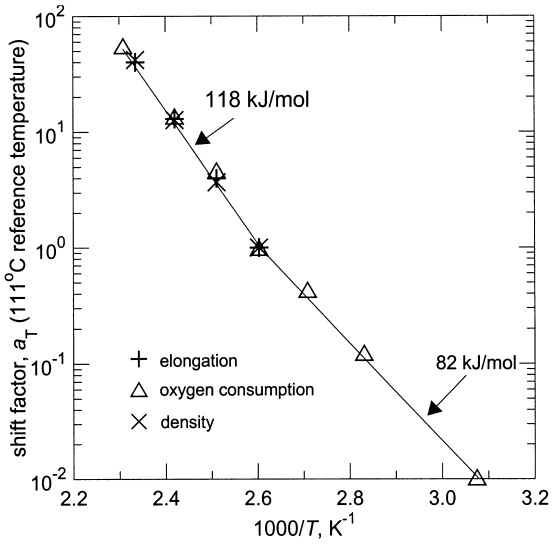

Fig. 20. Arrhenius plot of shift factors obtained from empirical time–temperature superposition of the indicated EPDM rubber degradation parameters.

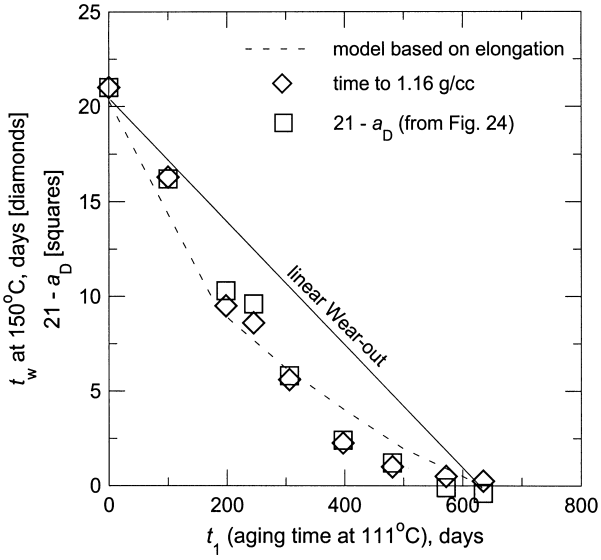

Fig. 21. Theoretical and experimental wear-out results for the EPDM material. Samples previously aged at 111°C were wear-out aged at 150°C.

density as our wear-out parameter. Another advantage of density is the dramatic induction-time behavior, implying that the point of failure should be relatively easy to determine. Since a density of 1.16 g/cc corresponds approximately to the elongation reaching ~50% (Figs. 16 and 22), we chose this value of density as our density failure criterion. Fig. 23 shows density results versus 150°C aging time for samples that had previously been aged for the indicated number of days at 111°C. The values of t_w required at 150°C for the density to reach 1.16 g/cc are plotted as diamonds versus the aging times at 111°C in Fig. 21. Although the experimental results are somewhat higher than the theoretical expectations for short 111°C aging times and somewhat below theoretical expectations at longer 111°C aging times, their overall behavior is in reasonable accord with the theoretical curve based on modeling the non-superposed elongation. Given the experimental scatter in the elongation and density results, the level of agreement is in fact encouraging.

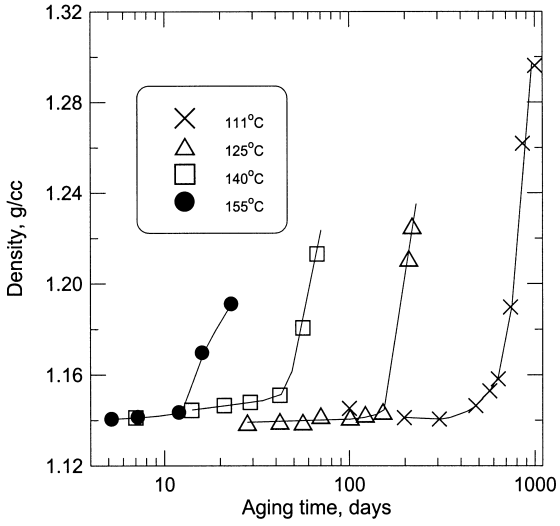

Fig. 22. Density results for the EPDM material versus aging time at the indicated temperatures.

If interactions are absent during the wear-out exposures, the shapes (on a linear time plot) of the degradation curves during the high temperature (150°C) exposures should be identical. This is obvious from Fig. 9, where the lack of interactions implies that regardless of the preaging time on the T_1 curve, all of the degradation curves for subsequent aging at T_2 (the Wear-out temperature) will superpose when translated horizontally to the T_2 curve. When interactions are present, it is clear from Fig. 10 that such superposition will not occur. Thus by attempting the time–degradation superposition procedure described earlier, we are able to test for the importance of interaction effects. In addition, this procedure uses all of the wear-out data instead of just a single processed point (e.g., the time required to reach a density of 1.16 g/cc).

Fig. 24 shows the results obtained from applying the time–degradation superposition procedure to the data of Fig. 23. The empirically derived additive shift factors (designated as a_D) that led to the best superposition are indicated on the figure, where the reference condition ($a_D = 0$) corresponds to the previously unaged material. The superposition is quite reasonable and offers evidence that important interaction effects are absent for the experimental conditions studied. Again, the advantages of the time–degradation superposition approach are that all of the data are used in the analyses and the importance of interaction effects can be assessed. To

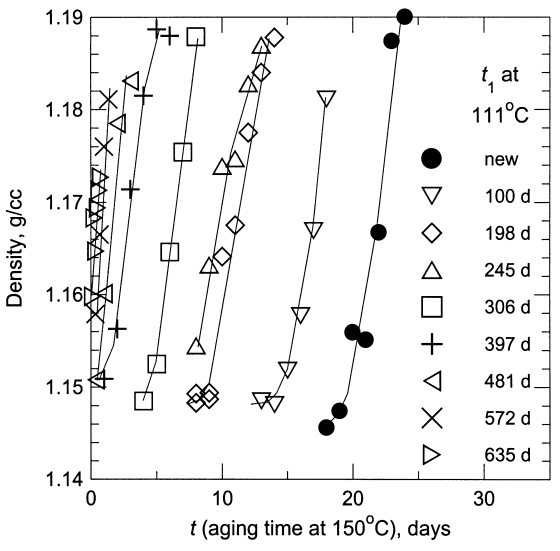

Fig. 23. Density results versus aging time at 150°C for the EPDM samples previously aged at 111°C for the indicated times.

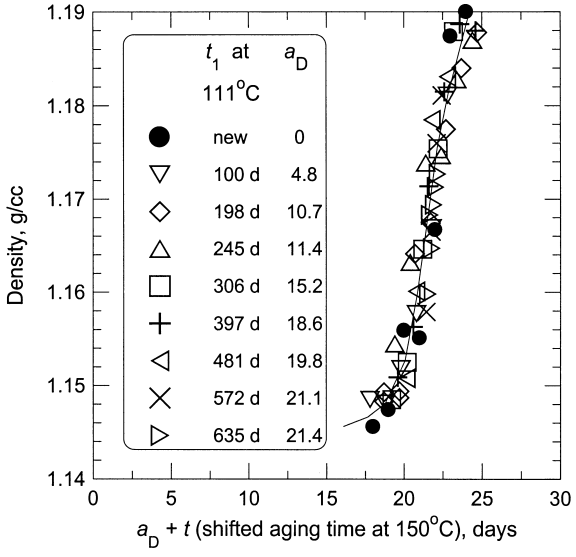

Fig. 24. Time–degradation superposition of the EPDM density results shown on Fig. 23.

utilize the derived shift factors for predicting remaining lifetime, we again select 1.16 g/cc as the failure criterion. From the superposed results of Fig. 24, we estimate that 21 days at 150°C are required to reach this condition for the previously unaged material. Thus a plot of $21-a_D$ versus aging time at 111°C (open squares) represents a Wear-out plot that is similar to the failure time plot (diamonds) of Fig. 21. The distinction would be that the experimental data come from time–degradation superposition (all of the data used) instead of from single processed points (the estimated failure times). The excellent agreement between the diamonds and the squares is not surprising given the observation of reasonable time-degradation superposition. It should be clear from the results in Figs. 21 and 22 that the wear-out approach now offers the opportunity for estimating the remaining lifetime of ambiently aged materials even for the most difficult cases where their degradation properties change very little until catastrophic failure (induction-time behavior).

As expected from the evidence suggesting a change in oxidation mechanism around 111°C (non time–temperature superposition of elongation, non-Arrhenius oxygen consumption), the experimental wear-out results of Fig. 21 are not linear. In fact, to a first approximation, they are in reasonable agreement with the curve crudely predicted earlier from modeling the elongation results (dashed curve of Fig. 21). Thus, as anticipated earlier, non time-temperature superposition (without interaction) similar to that shown in Fig. 8 should generally correspond to a wear-out plot similar to curve II of Fig. 7. In such instances, early wear-out results will give conservative (less than actual) predicted lifetimes. As wear-out results are later obtained for samples preaged for longer times at the lower temperature, lifetime estimates will progressively increase.

3.5. General comments on using and applying the wear-out approach

It is easy to see from the discussion and the experimental results given above that linear wear-out results will not always occur. However, applying the wear-out method for predicting remaining life involves periodically generating wear-out results on ambiently aged material as a function of time under ambient conditions. Early results would allow initial estimates of remaining life by assuming linear extrapolation behavior. As more data became available, more refined and confident extrapolations could be made.

An important consideration in choosing the wear-out temperature (T_w) for such experiments is minimizing the temperature difference between the temperature of interest and T_w. This is obvious for several reasons. First and foremost, the likelihood for acceptable time–temperature superposition of the degradation variables and therefore reasonably linear wear-out behavior, is increased if the temperature difference is minimized, since a larger temperature difference increases the chance for a change in the chemical degradation mechanism. In addition, keeping T_w as low as possible reduces the chances of physical complications such as diffusion-limited oxidation effects. Opposing the desire to keep T_w as low as practical is the need to complete the wear-out experiments in a reasonable time period. Balancing these two contradictory requirements leads to the conclusion that T_w should be selected such that degradation is completed over a few weeks to a few months time frame.

By periodically obtaining additional ambiently aged samples of increasing age, future wear-out experiments can be used to generate more data, leading to refined and more confident lifetime estimates. Of course, by definition, we do not have the complete degradation curve under ambient conditions. Therefore we do not have explicit evidence that the ambient degradation would time–temperature superpose with degradation at the wear-out temperature, a forecaster of linear wear-out behavior. In fact, we will never have such evidence in the absence of the complete ambient data up to failure. But, if we have confirmed time–temperature superposition from careful accelerated experiments, there would be a reasonable chance that this superposition will remain valid down to ambient conditions. This implies that wear-out experiments on the long-term, ambiently aged samples could give reasonably linear behavior. The key is that wear-out experiments versus ambient aging time will allow us to check the linearity of the results and whether the predicted failure time from extrapolation of the wear-out data is consistent with the failure time predicted from extrapolation of conventional accelerated aging results. In cases when linear wear-out behavior does not hold (Fig. 21), periodic estimates of the remaining lifetime can still be made and later refined as data on older samples is collected and added to the plot.

It is important to note that it is not necessary to obtain an unaged sample in order to make remaining lifetime predictions, as long as real-time aged samples of differing ages are available to allow the shape of the wear-out plot to be followed and extrapolated. This is significant since it may not always be possible to obtain an unaged sample 15 or 20 years after the material of interest is placed into use. This observation, in fact, constitutes another advantage of the wear-out approach relative to other lifetime prediction methods.

Notice also, that to utilize the wear-out approach, we do not have to explicitly know how the damage parameter depends on time at a constant temperature. It could have linear Palmgren–Miner dependence or any other shape, such as the three example curves in Fig. 5. If we have unaged material to evaluate, experiments on

this material at the wear-out temperature will allow us to determine the shape of the damage parameter versus time at the wear-out temperature. The shape could, of course, be the same or different under low temperature ambient conditions dependent upon whether time–temperature superposition holds. An interesting situation occurs if a degradation parameter can be found that appears to follow linear P–M behavior under accelerated conditions. In this case, simply following the degradation parameter versus field aging time may also yield linear results assuming time–temperature superposition is valid down to ambient conditions. If the observed linearity under ambient conditions is assumed to continue till failure, simply following the degradation parameter and extrapolating its values to its failure value offers a direct method of predicting remaining lifetime. Full-scale wear-out experiments like those described above would not be necessary in this situation.

Unfortunately, it is rather unusual to find linear Palmgren–Miner behavior for polymer degradation parameters. Although most studies have examined degradation behavior under laboratory (accelerated) conditions, if linear behavior was observed under such conditions, there would be a reasonable chance (if time–temperature superposition holds) that similar linear behavior would occur at ambient temperatures. We showed above that density for EPDM materials tends to follow "induction time" behavior (Fig. 22). For the nitrile material, density gave reasonably linear behavior over the mechanical property lifetime (Fig. 12). For this material, the relatively linear behavior of density is consistent with the observation that the isothermal oxygen consumption rates are relatively constant versus aging time (Fig. 1). Linear density behavior has also been observed for thermal aging of a PVC cable jacketing material at 110°C [18]. On the other hand, induction-time behavior similar to that found for the EPDM materials has been observed from density measurements for additional EPDM materials and for cross-linked polyolefin and chlorosulfonated polyethylene materials [18].

4. Conclusions

In summary, our proposed wear-out methodology represents an excellent approach for predicting the useful lifetime of polymers at any service temperature of interest. The method relies on the experimental completion of aging (wear-out) to a selected failure criterion at elevated temperatures and is based on cumulative damage concepts. The approach can transform very non-linear degradation results (e.g. induction-time behavior) into results that are much more amenable to predictive extrapolations. To better analyze wear-out results, we introduce a concept that we refer to as time–degradation superposition. This approach not only uses all of the aging data instead of a few processed data points but also allows one to examine the potential importance of interaction effects. Experimental wear-out results on two materials are utilized to show the potential utility of the approach.

Acknowledgements

Sandia is a multiprogram laboratory operated by Sandia Corporation, a Lockheed Martin Company, for the United States Department of Energy under Contract DE-AC04-94AL85000. The authors gratefully acknowledge able experimental assistance from G.M. Malone (elongation, density and modulus measurements), J. Wise (oxygen consumption experiments) and A.C. Graham (oxygen consumption and density measurements).

References

[1] Gillen KT, Celina M, Clough RL, Wise J. Trends in Polym Sci 1997;5:250.
[2] Palmgren A. Z Vereins Deutscher Ingenieure 1924;68:339.
[3] Miner MA. J Appl Mech 1945;A159.
[4] Wise J, Gillen KT, Clough RL. Polym Degrad Stab 1995;49:403.
[5] Anon. ASTM Standard D792-91. Density and specific gravity of plastics by displacement.
[6] Celina M, Gillen KT, Wise J, Clough RL. Radiat Phys Chem 1996;48:613.
[7] Gillen KT, Clough RL, Quintana CA. Polym Degrad Stab 1987;17:31.
[8] Kelen T. Polymer degradation. Van Nostrand Reinhold, 1983.
[9] Bolland JL. Proc R Soc London 1946;A186:218.
[10] Bateman LQ. Rev (London) 1954;8:147.
[11] Wise J, Gillen KT, Clough RL. Polymer 1997;38:1929.
[12] Ferry JD. Viscoelastic properties of polymers. John Wiley and Sons, 1970.
[13] Hwang W, Han KS. J Compos Mater 1986;20:125.
[14] Cunliffe AV, Davis A. Polym Degrad Stab 1982;4:17.
[15] Gillen KT, Clough RL. Polymer 1992;33:4358.
[16] Clough RL, Gillen KT. Polym Degrad Stab 1992;38:47.
[17] Gillen KT, Clough RL. In: Cheremisinoff NP, editor. Handbook of polymer science and technology, vol. 2. New York: Marcel Dekker, 1989. p. 167.
[18] Gillen KT, Celina M, Clough RL. Radiat Phys Chem 1999;56:429.